Department of AERONAUTICS and ASTRONAUTICS
STANFORD UNIVERSITY

AMES
GRANT
IN-24-CR
233346
24 P.

Final Report to
NASA Ames Research Center
Grant No. NCA2-311

DELAMINATIONS IN COMPOSITE PLATES CAUSED BY NON-PENETRATING IMPACT

Scott R. Finn and George S. Springer
Department of Aeronautics and Astronautics
Stanford University, Stanford, California 94305

(NASA-CR-185063) DELAMINATIONS IN COMPOSITE PLATES CAUSED BY NON-PENETRATING IMPACT Final Report (Stanford Univ.) 24 pCSCL 11D

N89-29493

Unclas
G3/24 0233346

October 1989

Final Report to
NASA Ames Research Center
Grant No. NCA2-311

DELAMINATIONS IN COMPOSITE PLATES CAUSED BY NON-PENETRATING IMPACT

Scott R. Finn and George S. Springer
Department of Aeronautics and Astronautics
Stanford University, Stanford, California 94305

October 1989

ABSTRACT

A model is presented for estimating the dimensions of delaminations in continuous fiber reinforced composite plates subjected to non-penetrating ("low velocity") impact of a solid object. The model is based on dimensional analysis, and results in two simple, closed form expressions, one providing the delamination length, the other the delamination width. Comparisons of delamination lengths and widths calculated by these expressions with experimental data suggest that the model predicts these dimensions with reasonable accuracy.

I. INTRODUCTION

Delaminations in composites caused by the impact of a solid object are of great practical concern. Delaminations may reduce significantly the strength and stiffness of the material, especially when the impacted laminate is under compression. Therefore, in order to utilize composites to their full advantage, we must be able to assess their susceptibility to impact. Specifically, it is important to know the locations and dimensions of delaminations which may occur due to impact.

Recently, Wu and Springer [1] described a method for estimating the locations and sizes of delaminations inside fiber reinforced organic matrix plates impacted by a solid object. Wu and Springer's analysis utilizes a three dimensional, transient, finite element stress analysis coupled with a failure criterion based on dimensional analysis. In addition to the delamination sizes and locations, this analysis also provides detailed behavior of the impactor and the impacted plate (e.g., displacement and velocity of the impactor, contact force as a function of time, and displacements, velocities, stresses and strains in the plate as functions of position and time). The disadvantage of the Wu-Springer analysis is that it requires long computation times on mainframe computers.

Frequently, in practice, the full history of the impactor and the plate is not needed; an estimate of the locations and sizes of the delaminations suffices. This investigation was undertaken to develop a method which provides this information simply and easily, without recourse to very long computer calculations. The present method is based on the failure criteria proposed by Wu and Springer, but does not require the time consuming finite element calculations. Instead, the method described in this paper results in closed form expressions, which readily yield the locations and sizes of delaminations caused by non-penetrating ("low velocity") impact.

II. THE PROBLEM

We consider a rectangular plate (thickness h) made of a continuous fiber-reinforced, organic matrix composite (Figure 1). The plate consists of n plies or lamina. The ply orientations are arbitrary and need not be symmetric with respect to the mid-surface of the plate. Perfect bonding between each ply is assumed.

The plate is supported along all four edges. Each edge may be either clamped or simply supported. A solid object of mass m, speed V, and "nose" radius r impacts the center of the plate (Figure 1). It is assumed that during impact the impactor does not penetrate the surface. The objective is to develop a method which can be used to estimate the locations and sizes of delaminations caused by the non-penetrating impact.

III. DELAMINATION

The shape of the delamination is irregular. However, previous data have shown the major axis of the delamination is, in general, parallel to the fiber direction of the lower ply [2]. Therefore, we characterize the delamination between any two plies by the length ℓ_D and width w_D which are taken to be the dimensions of the delamination in the directions parallel and perpendicular to the fiber direction in the lower ply, i.e., in the ply further from the impactor (Figure 2).

By using dimensional analysis, Wu and Springer [1] obtained the following expressions for the delamination lengths and widths

$$\frac{\ell_D}{\ell_0} = C_1 \left(\frac{\sigma_{\max}\sqrt{\ell_0}}{K_{Ic}} \right)^{C_2} (Q^*)^{C_3} \left(\frac{t_f}{t_m} \right)^{C_4} \left(\frac{D^B_{\theta\theta}}{D^T_{\theta\theta}} \right)^{C_5} \tag{1}$$

$$\frac{w_D}{\ell_0} = C_6 \left(\frac{\sigma_{\max}\sqrt{\ell_0}}{K_{Ic}} \right)^{C_7} (Q^*)^{C_8} \left(\frac{t_f}{t_m} \right)^{C_9} \left(\frac{D^B_{\theta\theta}}{D^T_{\theta\theta}} \right)^{C_{10}} \tag{2}$$

K_{Ic} and ℓ_0 are ply properties which must be determined by tests. K_{Ic} is the Mode I critical stress intensity factor (opening mode). ℓ_0 is the critical crack length given by

transverse tensile strength measurements [1, 3]

$$\ell_0 = \frac{2K_{Ic}^2}{\pi S_{TT}^2} \tag{3}$$

where S_{TT} is the transverse ply tensile strength.

Q^* and $D_{\theta\theta}$ are laminate properties which can be calculated from laminated plate theory. Q^* is proportional to the difference between the stiffnesses of the two plies adjacent to the delamination in the direction of the fibers of the "lower" ply (Figure 2). The parameter Q^* is defined as:

$$Q^* \equiv \frac{Q_{zz}^{\ell} - Q_{\theta\theta}^{u}}{Q_{zz}^{\ell} - Q_{yy}^{u}} \tag{4}$$

Q_{zz} and Q_{yy} are the reduced stiffnesses parallel and perpendicular to the fibers. $Q_{\theta\theta}$ is the transformed reduced stiffness corresponding to the angle θ between the fiber orientations of the two plies adjacent to the delamination (Figure 2). The superscripts ℓ and u refer to the lower and upper plies. For convenience, an expression for Q^* in terms of the ply properties and the angle θ is given in the Appendix.

$D_{\theta\theta}^T$ and $D_{\theta\theta}^B$ are the flexural rigidities of the sections of the laminate above and below the delamination, respectively, in the direction of the fibers of the ply immediately below the delamination (Figure 2). These values can be found by considering the two sections as separate laminates and calculating their flexural rigidities according to [4]

$$D_{\theta\theta} = \int Q_{\theta\theta}\, z^2\, dz \tag{5}$$

where $Q_{\theta\theta}$ is the same as previously given, and z is measured from the midplane of the individual section, not of the entire laminate.

The remaining three parameters $\sigma_{\max}$, t_m, and t_f depend on the laminate as well as on the impact. $\sigma_{\max}$ is the maximum out-of-plane tensile stress under the point of impact. t_m is the time at which this stress occurs. Finally, t_f is the duration of the stress. Wu and Springer [1] evaluated $\sigma_{\max}$, t_f, and t_m using a three-dimensional, transient, finite element method. Here, our analysis differs from that of Wu and Springer. We propose to approximate these three parameters in a simple manner, as described below.

The maximum stress σ_{max} is taken to be proportional to the pressure P which arises at the flat interface of two elastic, semi-infinite cylinders when the two cylinders collide

$$\sigma_{max} \equiv k_1 P \tag{6}$$

where k_1 is a constant. The impact pressure P is given by [5]

$$P = \frac{\rho_i V c_i}{1 + \frac{\rho_i c_i}{\rho_c c_c}} \tag{7}$$

where V is the relative velocity between the two impacting surfaces, which, in our case, is the impact velocity, ρ is the density, and c is the dilatational wave speed in the material. The subscripts i and c refer to the impactor and the impacted cylinder, respectively. In our problem, the latter corresponds to the top ply of the composite plate. Thus, the wave speeds in the impactor and in the impacted composite may be calculated by the expressions

$$c_i = \sqrt{E_i/\rho_i} \qquad c_c = \sqrt{E_{yy}/\rho_c} \tag{8}$$

where E_i is the Young's modulus of the impactor, and E_{yy} is the transverse ply modulus of the composite.

The time t_m required to reach σ_{max} is taken to be proportional to the time it takes for the first wave (caused by the impact) to travel in the composite from the impact surface to the back surface of the laminate. Thus, we write

$$t_m = k_2 t_w \tag{9}$$

and

$$t_w = h/c_c \tag{10}$$

where k_2 is a proportionality constant and h is the thickness of the laminate. For plates made of sublaminates of different materials, this expression can be generalized to

$$t_w = \sum_{j=1}^{n} \frac{h^{(j)}}{c_c^{(j)}} \tag{11}$$

where $h^{(j)}$ is the thickness of the j^{th} sublaminate, $c_c^{(j)}$ is the wave speed in the material of that sublaminate, and n is the total number of sublaminates.

The duration of the stress t_f is approximated by the time during which the impactor is in contact with the impacted surface.

$$t_f = t_{ct} \tag{12}$$

This contact time is taken to be proportional to the contact time for the one-dimensional problem of a rigid body of mass m impacting a massless, elastic cylinder of length h and diameter $2r$ (twice the nose radius of the actual impactor).

$$t_{ct} = k_3\, t_{1D} \tag{13}$$

For the one-dimensional problem the contact time is [6]

$$t_{1D} = \frac{\pi h}{c_c}\left(\frac{m}{\pi r^2 h \rho_c}\right)^{1/2} \tag{14}$$

For plates with sublaminates of different materials, the corresponding equation is

$$t_{1D} = \left[\frac{\pi m}{r^2}\sum_{j=1}^{n}\frac{h^{(j)}}{(c_c^{(j)})^2 \rho_c^{(j)}}\right]^{1/2} \tag{15}$$

where $h^{(j)}$, $c_c^{(j)}$, $\rho_c^{(j)}$ are the thickness, wave speed, and density of the j^{th} sublaminate, respectively.

By substituting Eqs. (6)–(14) into Eqs. (1) and (2) we obtain

$$\frac{\ell_D}{\ell_0} = A\left(\frac{P\sqrt{\ell_0}}{K_{Ic}}\right)^{C_2}(Q^*)^{C_3}\left(\frac{t_{1D}}{t_w}\right)^{C_4}\left(\frac{D_{\theta\theta}^B}{D_{\theta\theta}^T}\right)^{C_5} \tag{16a}$$

$$\frac{w_D}{\ell_0} = B\left(\frac{P\sqrt{\ell_0}}{K_{Ic}}\right)^{C_7}(Q^*)^{C_8}\left(\frac{t_{1D}}{t_w}\right)^{C_9}\left(\frac{D_{\theta\theta}^B}{D_{\theta\theta}^T}\right)^{C_{10}} \tag{16b}$$

A and B are constants

$$A = k_1^{C_2}\left(\frac{k_3}{k_2}\right)^{C_4} C_1 \tag{17}$$

$$B = k_1^{C_7}\left(\frac{k_3}{k_2}\right)^{C_9} C_2 \tag{18}$$

The constants A, B, C_2–C_5, and C_7–C_{10} must be obtained by fitting Eqs. (16a) and (16b) to experimentally determined delamination lengths and widths. Therefore, we performed a least squares fit of these equations to the data given in Reference 2 and summarized

in Tables 1 and 2. This procedure yielded the following values

$$\begin{aligned} A &= 180 \qquad B = 20 \\ C_2 &= 3/4 \qquad C_7 = 4/3 \\ C_3 &= 1/2 \qquad C_8 = 4/3 \\ C_4 &= 1/4 \qquad C_9 = 1/3 \\ C_5 &= 2/5 \qquad C_{10} = 0 \end{aligned} \tag{19}$$

For these values, the expressions for the delamination length and width become

$$\frac{\ell_D}{\ell_0} = 180 \left(\frac{P\sqrt{\ell_0}}{K_{Ic}} \right)^{3/4} (Q^*)^{1/2} \left(\frac{t_{1D}}{t_w} \right)^{1/4} \left(\frac{D_{\theta\theta}^B}{D_{\theta\theta}^T} \right)^{2/5} \tag{20}$$

$$\frac{w_D}{\ell_0} = 20 \left(\frac{P\sqrt{\ell_0}}{K_{Ic}} \right)^{4/3} (Q^*)^{4/3} \left(\frac{t_{1D}}{t_w} \right)^{1/3} \tag{21}$$

As previously discussed, the multipliers (180 and 20) as well as the exponents are constants independent of material property, layup, and impact velocity.

IV. CALCULATION PROCEDURE

By using Eqs. (20) and (21) the delamination length and width can be estimated between any two plies in the plate. To perform the calculations we must first select the location (or locations) at which we wish to determine the dimensions of the delaminations. At each location of interest the delamination length and width are calculated by Eqs. (20) and (21).

The parameters K_{Ic} and ℓ_0 are material properties and their values must be determined by static tests (Eq. 3). The value of Q^* depends on the material, on the layup, and on the location under consideration, and can be calculated by Eq. (4). The flexural rigidities $D_{\theta\theta}^T$ and $D_{\theta\theta}^B$ depend on the material and on the layup and can be calculated by Eq. (5). Note that the location of the delamination is taken into account through $D_{\theta\theta}^T$ and $D_{\theta\theta}^B$. The impact pressure P, the duration of the stress t_{1D}, and the time t_w required to reach the maximum stress depend on the material, the layup, and on the impact, and are to be calculated by Eqs. (7), (10), and (14).

The calculations can be performed readily by a personal computer or even on a programmable calculator. To perform the calculations we have written a computer code (designated as "SIMPACT"). The input parameters required by the code are given in Table 3.

V. DISCUSSION

To illustrate the use of Eqs. (20) and (21), delamination lengths and widths were calculated for the conditions which existed in the tests reported in Reference 2 and summarized in Tables 1 and 2. Essentially, in these tests, Fiberite T300/934 graphite epoxy plates (16 plies thick, 4 in by 4 in) were impacted by 1/2 in diameter aluminum spheres [2]. The plates were inspected by an ultrasonic scanning technique (C-scan) before and after impact. After impact the plates were also cut along their axes of symmetry, and were examined by an optical microscope. The measured shapes of the delaminations are shown as solid lines in Figures 3–6. Delaminations lengths and widths were also calculated by the model (Eqs. 20 and 21) using the material properties listed in Table 4. The results of the calculations are indicated by dotted lines. The comparisons in these figures show that the calculated and measured delamination lengths and widths agree closely.

A more quantitative assessment of the accuracy of the model can be made by comparing directly calculated delamination lengths with measured delamination lengths and calculated delamination widths with measured delamination widths. Such comparisons are made in Figures 7 and 8 and in Tables 1 and 2. Ideally, all the data should fall on the 45 degree solid lines. Deviations from these lines may be due to errors either in measurements or in the model. It is encouraging that the measured and estimated delamination dimensions agree within 25 percent for both the length and the width.

The foregoing results indicate that the present model can be used to estimate the lengths and widths of delaminations under a wide range of conditions. It is hoped that future tests will verify the model also to be valid under as yet untested conditions.

VI. REFERENCES

1. Wu, H. T. and Springer, G. S. "Impact Induced Stresses, Strains, and Delaminations in Composite Plates," *Journal of Composite Materials, Vol. 22, No. 6,* June 1988, pp. 533–560.
2. Wu, H. T. and Springer, G. S. "Measurements of Matrix Cracking and Delamination Caused by Impact on Composite Plates," *Journal of Composite Materials, Vol. 22, No. 6,* June 1988, pp. 518–532.
3. Broek, D. *Elementary Engineering Fracture Mechanics,* Martinus Nijhoff Publishers, the Hague, the Netherlands, 1986.
4. Tsai, S. W. *Composites Design,* Think Composites, Dayton, Ohio, 1987.
5. Springer, G. S. *Erosion by Liquid Impact,* Scripta Publishing Co., Washington, DC, 1976.
6. Timoshenko, S. P. and Goodier, J. N. *Theory of Elasticity,* McGraw-Hill, New York, 1970.
7. Jones, R. M. *Mechanics of Composite Materials,* Scripta Publishing Co., Washington, DC, 1975.
8. Johannesson, T. R. and Blikstad, M. "Mixed Mode Fracture of Grapphite/Epoxy Laminates," Proceedings of the International Symposium of Composite Materials and Structures, Technomic, Lancaster, PA, 1986.

APPENDIX
EXPRESSION OF THE REDUCED STIFFNESS MATRIX Q

The components of the reduced stiffness matrix Q are [7]

$$Q_{xx} = \frac{E_{xx}}{1 - \nu_{xy}\nu_{yx}} \tag{A.1}$$

$$Q_{xy} = \frac{\nu_{xy}E_{yy}}{1 - \nu_{xy}\nu_{yx}} \tag{A.2}$$

$$Q_{yy} = \frac{E_{yy}}{1 - \nu_{xy}\nu_{yx}} \tag{A.3}$$

$$Q_{ss} = G_{xy} \tag{A.4}$$

$$Q_{\theta\theta} = Q_{xx}\cos^4\theta + 2(Q_{xy} + 2Q_{ss})\sin^2\theta\cos^2\theta + Q_{yy}\sin^4\theta \tag{A.5}$$

where E_{xx} is Young's modulus in fiber direction, E_{yy} is Young's modulus transverse to fiber direction, ν_{xy} and ν_{yx} are Poisson's ratios, and G_{xy} is the shear modulus.

By substituting the appropriate expressions for Q_{xx}, Q_{yy}, and $Q_{\theta\theta}$, we obtain

$$Q^* = \frac{Q^l_{xx} - [Q^u_{xx}\cos^4_\theta + 2(Q^u_{xy} + 2Q^u_{ss})\sin^2\theta\cos^2\theta + Q^u_{yy}\sin^4\theta]}{Q^l_{xx} - Q^u_{yy}} \tag{A.6}$$

The superscripts l and u refer to the lower and upper plies, respectively.

Table 1

SUMMARY OF DELAMINATION LENGTHS OBTAINED BY C-SCAN AND CALCULATED BY THE PRESENT STUDY

Lay-Up	Boundary Conditions	Impact Velocity (in/sec)	Delamination Length (C-scan) (in)	Delamination Length (calculated) (in)	Location (ply # from the top)
$[0_{16}]$	clamped	1021	0.00	0.00	everywhere
		1263	0.00	0.00	
		1320	0.00	0.00	
$[0_4/90_8/0_4]$	simply supported	795	1.20	1.33	between #12 and #13
		1071	1.55	1.66	
		1306	1.70	1.93	
$[0_4/90_8/0_4]$	clamped	769	1.25	1.30	between #12 and #13
		1026	1.50	1.61	
		1307	2.10	1.93	
$[0_3/90_{10}/0_3]$	clamped	1037	0.85	1.09	between #13 and #14
$[0_2/90_{12}/0_2]$	clamped	1002	0.70	0.66	between #14 and #15
$[0_4/-45_4/45_4/90_4]$	clamped	774	1.60	1.64	between #12 and #13
		1008	2.00	2.00	
		1277	2.30	2.39	
$[0_4/45_4/60_4/90_4]$	clamped	775	1.10	1.01	between #12 and #13
		1050	1.15	1.27	
		1250	1.30	1.45	

Table 2

SUMMARY OF DELAMINATION WIDTHS OBTAINED BY C-SCAN AND CALCULATED BY THE PRESENT STUDY

Lay-Up	Boundary Conditions	Impact Velocity (in/sec)	Delamination Width (C-scan) (in)	Delamination Width (calculated) (in)	Location (ply # from the top)
$[0_{16}]$	clamped	1021 1263 1320	0.00 0.00 0.00	0.00 0.00 0.00	everywhere
$[0_4/90_8/0_4]$	simply supported	795 1071 1306	0.50 0.75 0.90	0.47 0.70 0.91	between #12 and #13
$[0_4/90_8/0_4]$	clamped	769 1026 1307	0.40 0.85 1.00	0.45 0.66 0.91	between #12 and #13
$[0_3/90_{10}/0_3]$	clamped	1037	0.60	0.67	between #13 and #14
$[0_2/90_{12}/0_2]$	clamped	1002	0.64	0.64	between #14 and #15
$[0_4/-45_4/45_4/90_4]$	clamped	774 1008 1277	0.32 0.47 0.66	0.30 0.43 0.59	between #12 and #13
$[0_4/45_4/60_4/90_4]$	clamped	775 1050 1250	0.15 0.25 0.30	0.15 0.22 0.28	between #12 and #13

Table 3

SUMMARY OF THE INPUT AND OUTPUT PARAMETERS FROM THE "SIMPACT" CODE

Input Parameters

1) Impactor
   a) Mass, m
   b) Nose radius, r
   c) Density, ρ_i
   d) Young's modulus, E_i
   e) Velocity, v

2) Composite Plate
   a) Ply layup
   b) Material properties (see Table 4)

Output Parameters

1) Final delamination length
2) Final delamination width

Table 4

MATERIAL PROPERTIES OF FIBERITE T300/934 GRAPHITE/EPOXY (from Reference 2).

Ply thickness, h	6.250×10^{-3}	in
Density, ρ	5.548×10^{-2}	lbm/in^3
Longitudinal Young's modulus, E_{xx}	2.109×10^7	psi
Transverse Young's modulus, E_{yy}	1.450×10^6	psi
Shear modulus in x-y direction, G_{xy}	8.251×10^5	psi
Poisson's ratio in the x-y direction,[a] ν_{xy}	0.3	
Transverse tensile strength, S_{TT}	8.006×10^3	psi
Critical stress intensity factor of mode I,[b] K_{Ic}	1.183×10^3	lbf/in$^{1.5}$

[a]From Reference 4.

[b]From Reference 8.

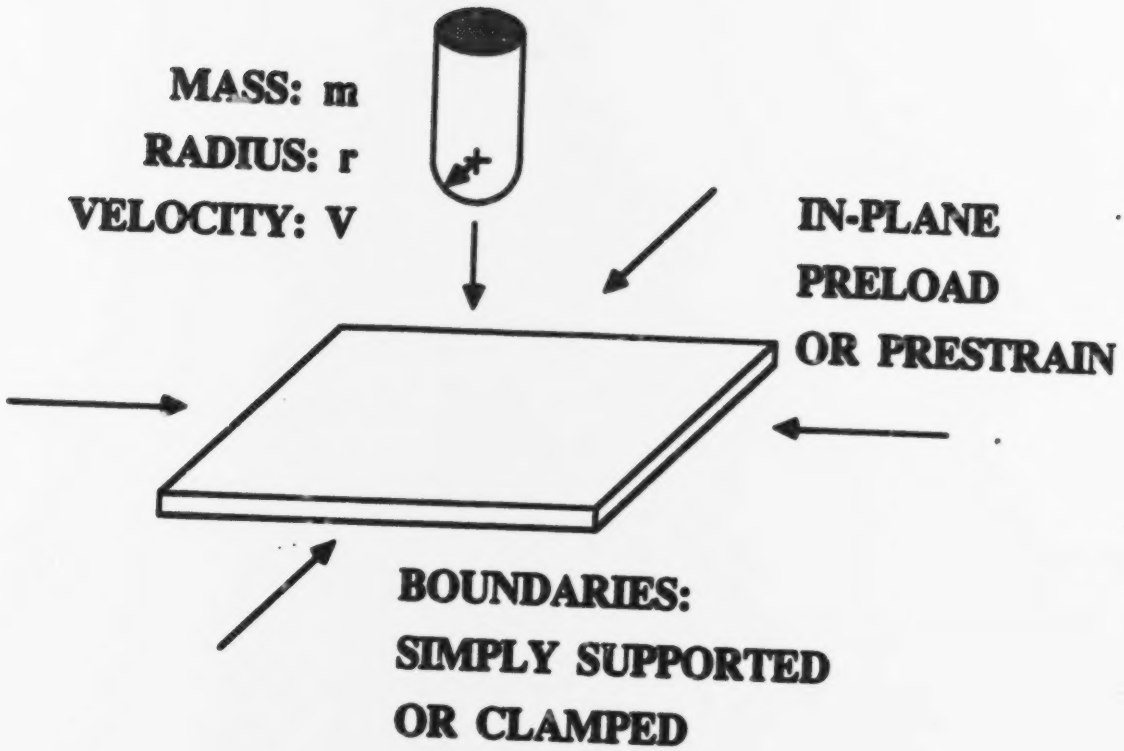

Figure 1. Description of the problem

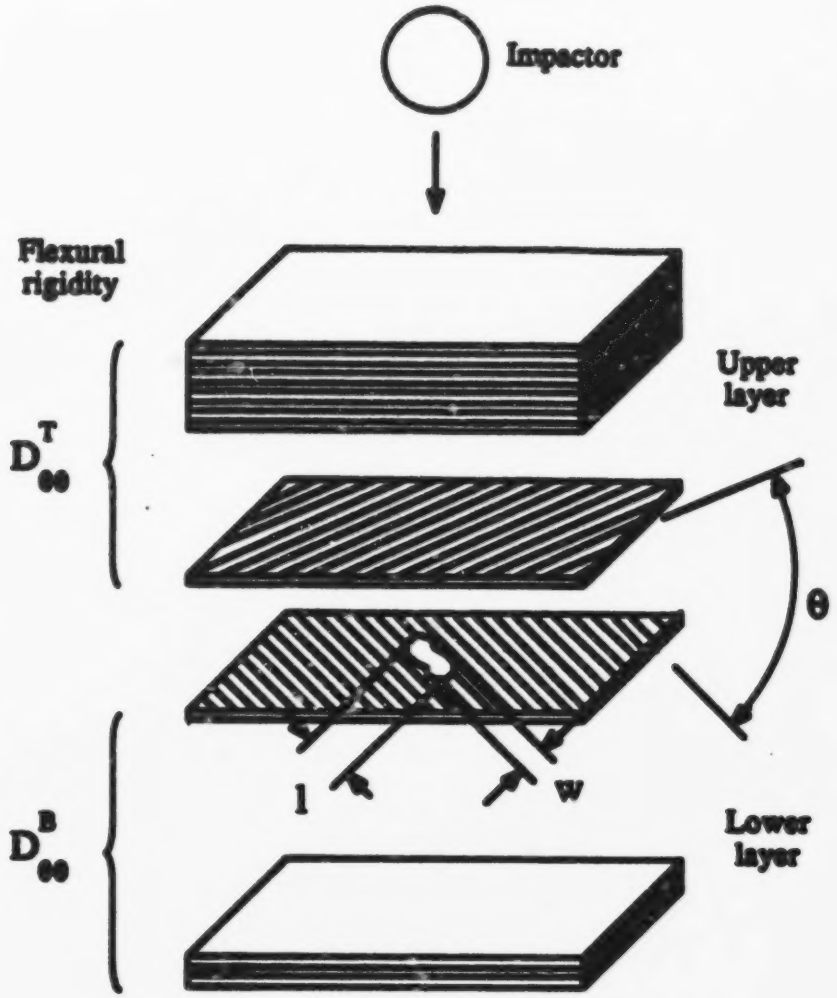

Figure 2. Illustration of the delamination

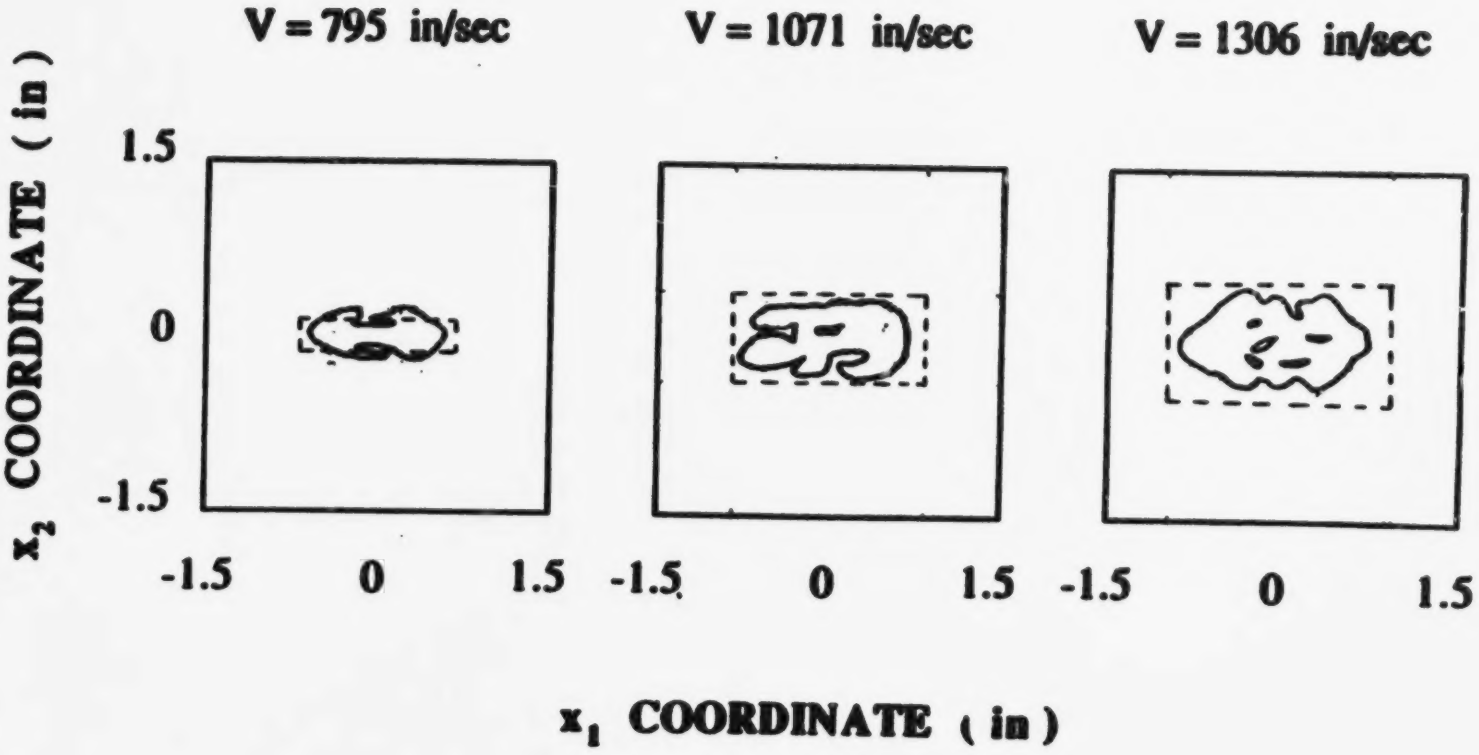

Figure 3. Comparison between the measured and calculated delaminations. Solid lines: measured by C-Scan [2]. Dotted line: calculated delaminations (eqs 20 and 21). T300/934 graphite/epoxy plates ($[0_4/90_8/0_4]$) with simply supported edges impacted by 1/2 inch diameter aluminum spheres.

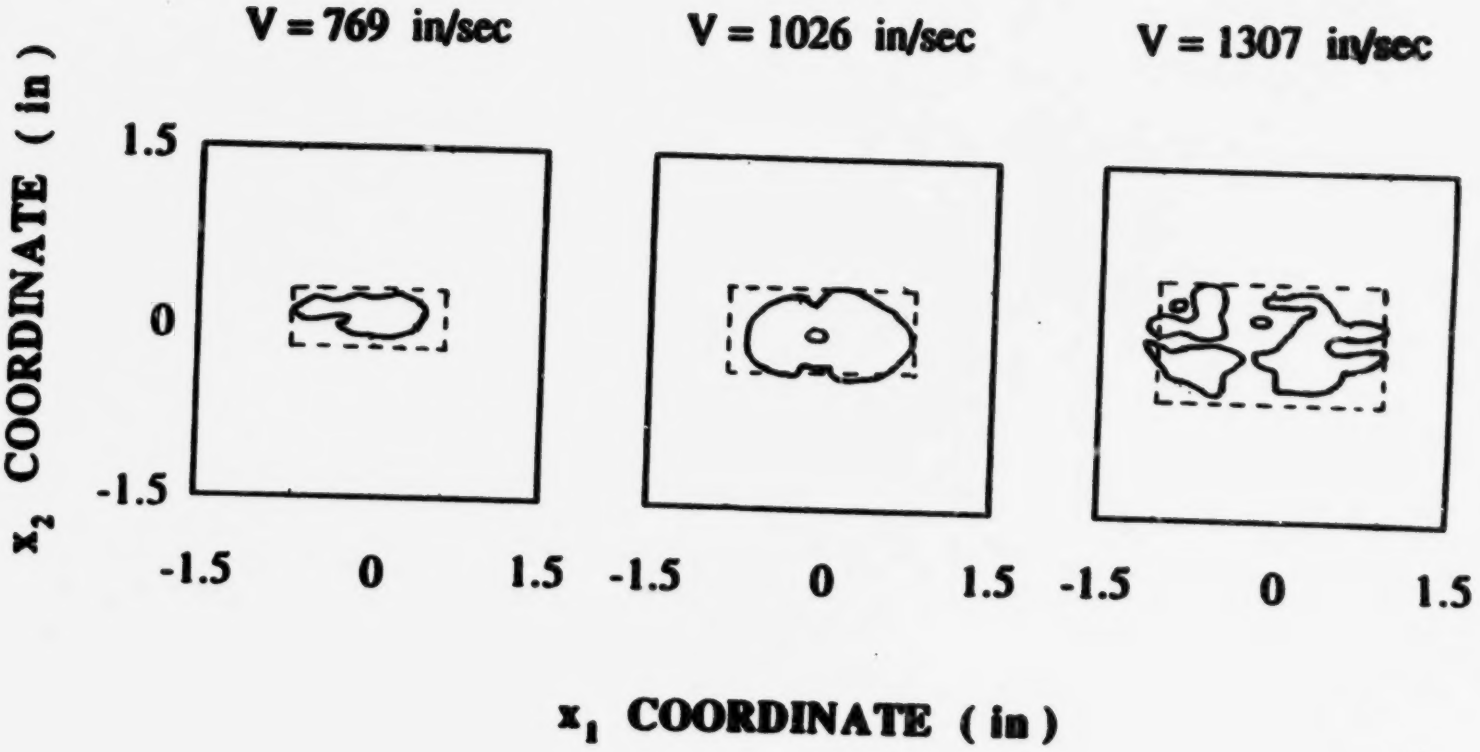

Figure 4. Comparison between the measured and calculated delaminations. Solid lines: measured by C-Scan [2]. Dotted line: calculated delaminations (eqs 20 and 21). T300/934 graphite/epoxy plates ($[0_4/90_8/0_4]$) with clamped edges impacted by 1/2 inch diameter aluminum spheres.

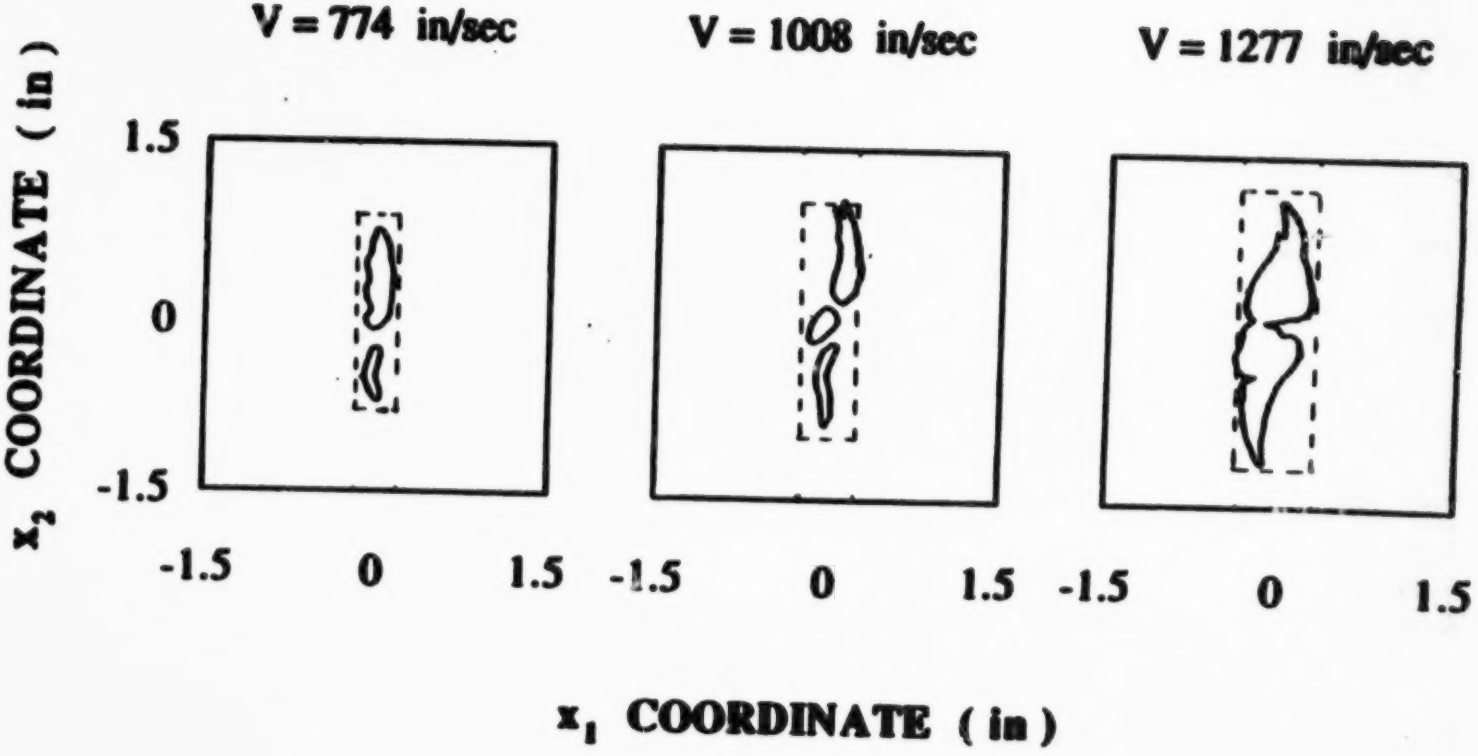

Figure 5. Comparison between the measured and calculated delaminations. Solid lines: measured by C-Scan [2]. Dotted line: calculated delaminations (eqs 20 and 21). T300/934 graphite/epoxy plates ($[0_4/-45_4/45_4/90_4]$) with clamped edges impacted by 1/2 inch diameter aluminum spheres.

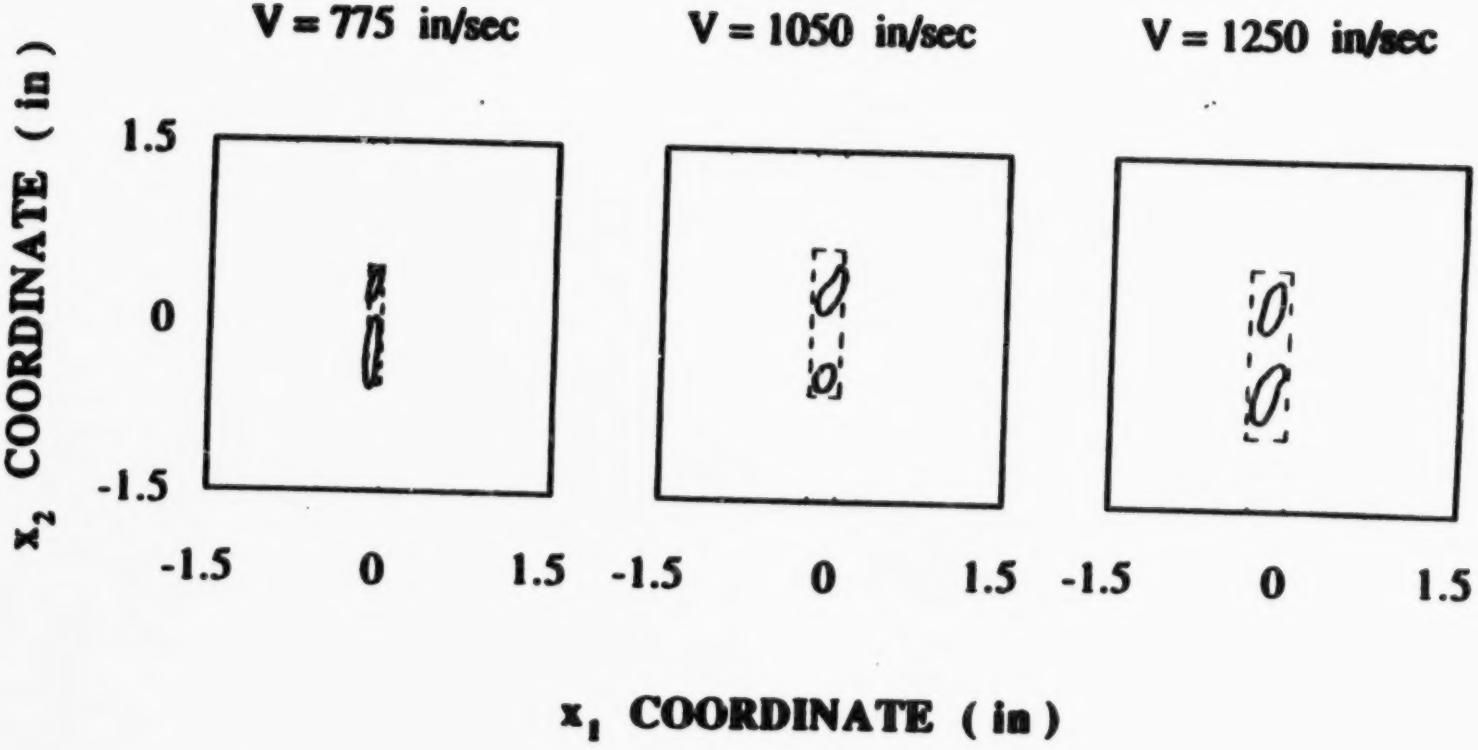

Figure 6. Comparison between the measured and calculated delaminations. Solid lines: measured by C-Scan [2]. Dotted line: calculated delaminations (eqs 20 and 21). T300/934 graphite/epoxy plates ($[0_4/45_4/60_4/90_4]$) with clamped edges impacted by 1/2 inch diameter aluminum spheres.

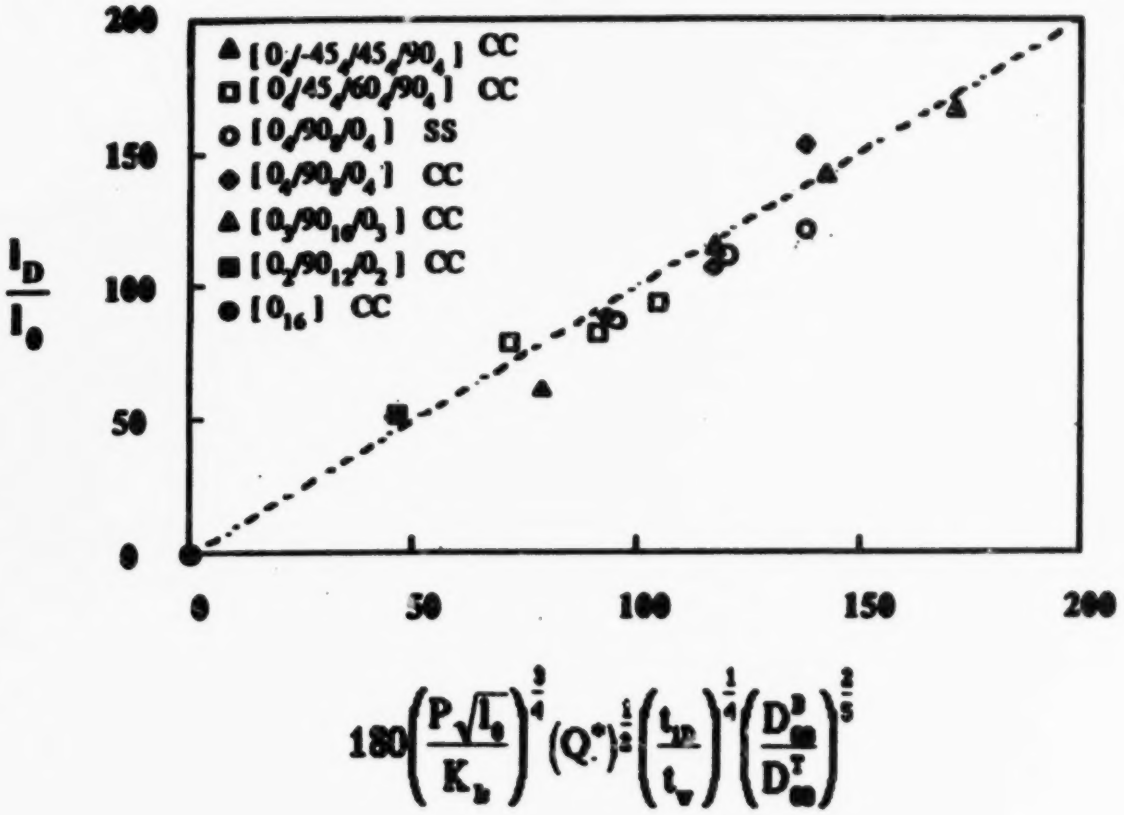

Figure 7. Delamination lengths in 3 inch by inch T300/934 graphite/epoxy plates impacted by 1/2 inch diameter aluminum spheres. Dotted line is the result of the least square fit of eq (20). SS: edges are simply supported; CC: edges are clamped.

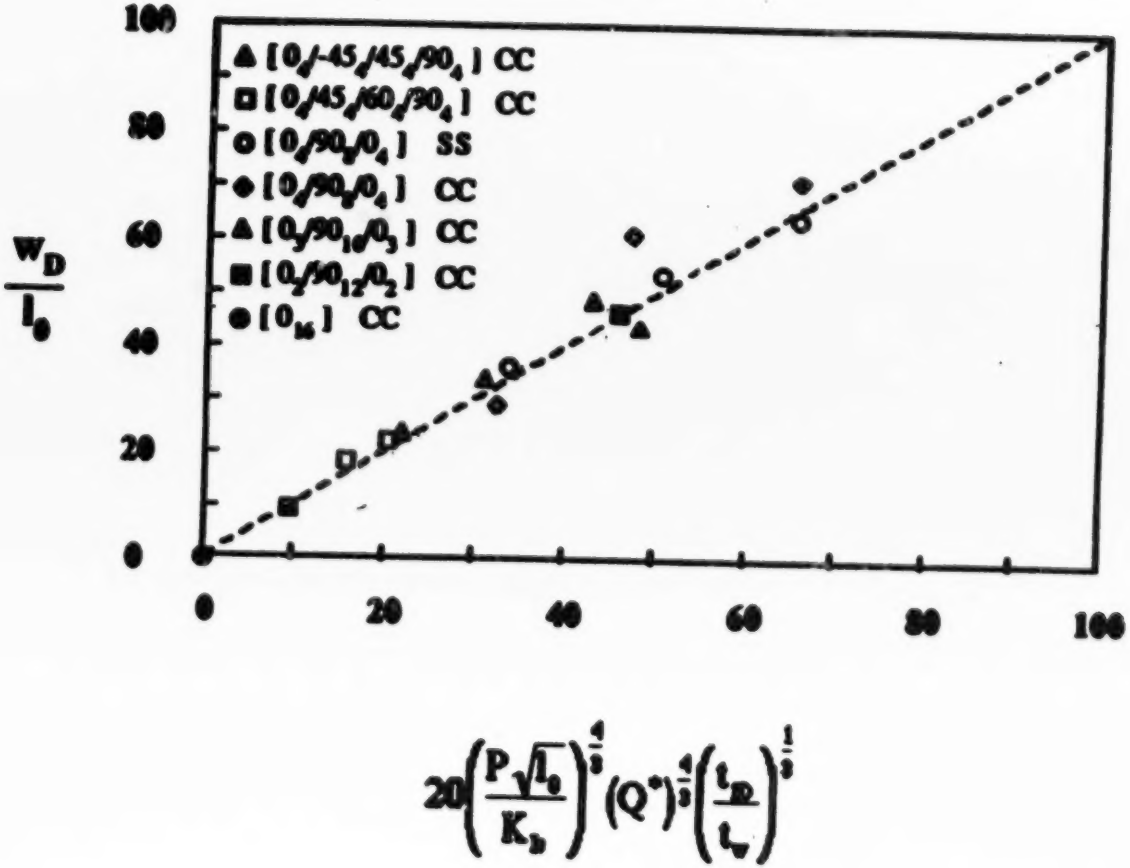

$$20\left(\frac{P\sqrt{l_0}}{K_b}\right)^{\frac{4}{3}}(Q^*)^{\frac{4}{3}}\left(\frac{t_{90}}{t_w}\right)^{\frac{1}{3}}$$

Figure 8. Delamination widths in 3 inch by inch T300/934 graphite/epoxy plates impacted by 1/2 inch diameter aluminum spheres. Dotted line is the result of the least square fit of eq (21). SS: edges are simply supported; CC: edges are clamped.